

UNIVERSIDAD DE CÓRDOBA

Facultad de Ciencias

Grado de Física

Trabajo Fin de Grado

# Baryon acoustic oscillations in a non-flat universe

Código del TFG: **FS22-17-FSC**

Tipo de TFG: **Trabajo teórico-práctico**

---

Autor: Santiago Sanz Wuhl



6 de Junio de 2023

---

## Agradecimientos

---

Agradecer antes que nada a mi familia; mi padre Fernando, mi madre Judith y mi hermana Sofi por apoyarme y lo que es más importante, soportarme todos estos años. Fuisteis el apoyo sin el cual no podría haber llegado hasta donde he llegado.

Por otro lado, a todos/as aquellos profesores que me motivaron a tomarme en serio esta carrera y seguir en el camino de la investigación, entre los cuales se encuentra y con razón, mi tutor Antonio J. Cuesta. Dentro del departamento, agradecer también al profesor Alberto Jiménez del Dpto. de Física de la Universidad de Córdoba el facilitarme el acceso a los ordenadores del grupo *FQM-378*.

Finalmente, agradecer a todas las personas que están detrás de este trabajo, desde la Universidad de Córdoba; Antonio J. Cuesta, Antonio Sarsa, y desde la Universidad de Barcelona, Héctor Gil-Marín y Licia Verde por ofrecer los códigos de análisis BRASS y RUSTICO utilizados en este trabajo de Fin de Grado.

---

## Contents

---

<b>Table of contents</b>	<b>2</b>
<b>List of figures</b>	<b>3</b>
<b>List of tables</b>	<b>4</b>
<b>Resumen. Palabras clave</b>	<b>5</b>
<b>Abstract. Keywords</b>	<b>6</b>
<b>1 Introduction</b>	<b>7</b>
1.1 The Hot Big Bang model . . . . .	7
1.2 Cosmic Microwave Background . . . . .	9
1.3 Baryon Acoustic Oscillations . . . . .	10
1.4 Curvature, dark matter and the expansion of the Universe . . . . .	12
1.5 $\Lambda$ Cold Dark Matter model . . . . .	16
<b>2 Objectives</b>	<b>19</b>
<b>3 Methods and materials.</b>	<b>20</b>
<b>4 Results</b>	<b>28</b>
<b>5 Conclusiones</b>	<b>32</b>
<b>5 Conclusions</b>	<b>34</b>
<b>Bibliografía</b>	<b>36</b>
<b>Appendix: Example of data visualisation code with python &amp; matplotlib</b>	<b>38</b>

---

# List of figures

---

1.1	The all-sky map of CMB anisotropies as seen by the Planck Satellite.	8
1.2	Different time evolution stages of the Baryon Acoustic Oscillations.	11
1.3	First BAO observations by the SDSS and the 2dF collaborations.	13
3.1	Power spectrum of the LRG eBOSS galaxies.	24
3.2	The template power spectrum, its smooth component and the pure BAO	24
3.3	The BAO analysis pipeline.	27
4.1	Derivation of cosmological distance measurements.	31

---

# List of Tables

---

1.1	Values of the fiducial cosmological parameters used in the BAO analysis and of the derived values $r_d$ , $D_H/r_d$ , $D_M/r_d$ , $\Omega_\Lambda$ , $\Omega_m$ . . . . .	18
4.1	Distance measurements to eBOSS galaxies for different assumed values of the curvature parameter $\Omega_k$ . . . . .	29

---

## Resumen

---

En este trabajo de fin de grado se hace uso de herramientas de computación de alto rendimiento y análisis de datos para estudiar los efectos de ligeras variaciones en el modelo cosmológico estándar, el modelo  $\Lambda$  *Cold Dark Matter* ( $\Lambda$ CDM). Este modelo asume un universo espacialmente plano, si bien las observaciones son compatibles con una curvatura no nula.

Este trabajo se basa en las oscilaciones acústicas de bariones, un fenómeno que nos permite estudiar el comportamiento del universo en sus etapas más tempranas (los primeros 380.000 años de sus 13.800 millones de años de vida, ¡un 0,003% de la vida del universo!). Estas oscilaciones dan forma a la estructura a gran escala del universo y, lo que es más importante, establecen una "regla cósmica"  $r_d$  con respecto a la cual se miden las distancias cosmológicas, como la distancia de Hubble  $D_H$  y la distancia del diámetro angular  $D_M$ .

Después de analizar el catálogo de galaxias del cartografiado *extended Baryon Oscillation Spectroscopic Survey*, obtenemos los siguientes resultados:  $D_H/r_d = 18.66 \pm 0.72$  y  $D_M/r_d = 18.28 \pm 0.53$  para un universo plano, en concordancia con los resultados para otros valores no nulos del parámetro de curvatura  $\Omega_k$  (hasta un 20% de la densidad total), y lo que es más importante, con resultados anteriores en el campo.

**Palabras clave:** Cosmología; Astrofísica; Oscilaciones Acústicas de Bariones; Análisis de datos.

---

## Abstract

---

In this Bachelor's Thesis we make use of high performance computing and data analysis tools to study the effects of slight variations in the Standard Cosmological model, the  $\Lambda$  Cold Dark Matter ( $\Lambda$ CDM) model. This model assumes a spatially flat universe, though the observations are compatible with a nonzero value of the curvature parameter  $\Omega_k$ .

This work is based off the Baryon Acoustic Oscillations, a phenomenon that allows us to study the behavior of the universe in its earliest stages (the first 380.000 of its 13.8 billion years of lifetime – a 0.003% of the Universe's lifetime!). These oscillations shape the large scale structure of the universe, and more importantly, set a 'cosmic ruler'  $r_d$  with respect to which is used to measure cosmological distances, such as the Hubble distance  $D_H$  and angular diameter distance  $D_M$ .

After analyzing the *extended Baryon Oscillation Spectroscopic Survey* galaxy catalogue, we achieve the following results:  $D_H/r_d = 18.66 \pm 0.72$  y  $D_M/r_d = 18.28 \pm 0.53$  for a flat universe, in concordance to the results for other nonzero values of the curvature parameter  $\Omega_k$  (up to a 20% of the total density), and more importantly with previous results in the field.

**Keywords:** Cosmology; Astrophysics; Baryon Acoustic Oscillations; Data Analysis.

## Introduction

---

### 1.1. The Hot Big Bang model

The most accepted model for the origin of the Universe is the Big Bang model, which models the beginning of the Universe as a hot dense state. The Big Bang surprisingly to some conveys no "bang", but the sudden existence of all the matter in the Universe, in the shortest of times, in the smallest of spaces, about 13.8 billion years ago. After an unthinkable small interval of time, the Universe began a short period of rapid expansion known as *cosmic inflation*, in which the Universe grew by a factor  $10^{27}$  in a mere  $10^{-33}$  seconds. This inflation is thought to be due to the inflaton, a quantum scalar field. It is theorized that it is the inflaton's vacuum energy what caused the Universe to expand as greatly.

As any quantum field<sup>1</sup> the inflaton presents fluctuations. This means, even in the vacuum state<sup>2</sup> there is constant creation and annihilation of virtual particles. These fluctuations are what cause anisotropies in the matter distribution of the Universe, fact that will be important later in this work.

---

<sup>1</sup>Quantum fields are a tool used by Quantum Field Theory (QFT) to more accurately describe particles and their interactions.

<sup>2</sup>To define vacuum in QFT is not as easy a task as it was in classical mechanics (or even non-relativistic quantum mechanics). These details go beyond the scope of this work, and thus will not be dealt with.



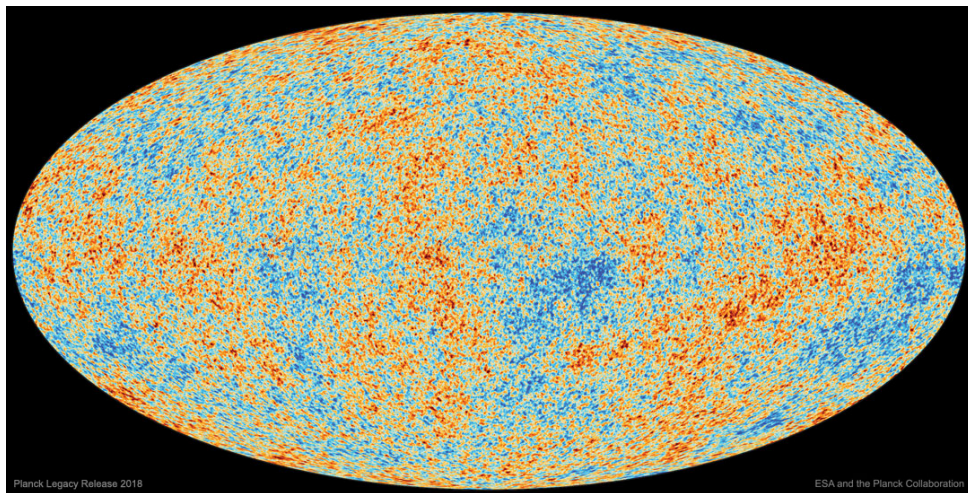


Figure 1.1: The all-sky map of CMB anisotropies as seen by Space-based Observatory Planck [1]. The colors in this map represent the fluctuations around the mean  $T = 2.7$  K with fluctuations of  $10^{-5}$  with respect to the average temperature. Red means higher temperature than the average, whilst blue means lower temperature than the average.

After the inflation phase, the Universe cooled enough for what is known as the Quark-Gluon plasma to form. In this state, temperatures were high enough as to consider relativistic the random motion of the particles in it. After some cooling due to cosmic expansion, the combination between quarks to form hadrons was allowed, leading to what is known as the hadronic epoch. However, due to the short mean free path of the photons, the Universe is still opaque to electromagnetic radiation.

As the Universe kept expanding the densities decreased and the temperatures cooled, the existence of atoms was starting to be allowed, the He and H atoms. This period would finish at the Universe age of 380,000 years, moment known as recombination. Recombination is thought of as the time at which the Thomson Scattering mechanisms stop being effective (the scattering cross section of this process becomes negligible and thus the photon mean free path grows considerably). As soon as recombination ends, the thermally activated photons which are no longer energetic enough to interact with the electrons now travel freely through space. This emission is known as the Cosmic Microwave Background (CMB) and is the oldest direct observation using electromagnetic radiation we can take of the Universe.

## 1.2. Cosmic Microwave Background

We see in the Fig. 1.1 the CMB as observed by the Planck collaboration [1]. The radiation we observe is the photons that were emitted about 13.8 billion years ago. Since the CMB appears as a result of the thermal photons emitted by the electrons in the primordial plasma, it offers great insight into what the plasma looked like, and the way it behaved.

The Cosmic Microwave Background was discovered in 1965 as a serendipity by Penzias and Wilson [2]. They observed a noise signal, uniformly distributed<sup>3</sup> from every direction, day or night, summer or winter, almost as if it came directly from the origin of the Universe. This discovery was considered to be solid evidence for the Big Bang model and more importantly, the beginning of the modern cosmology. All of this became the reason Penzias and Wilson received a Nobel prize 13 years later, in 1978.

Since what is being measured are the photons left from recombination, which corresponds to a thermal radiation curve, we may use Wien's displacement law

$$T = \frac{b}{\lambda} \quad (1.1)$$

with  $b \approx 2.897$  mm K Wien's constant,  $T$  the black body radiation and  $\lambda$  the wavelength at which the spectral radiation intensity is maximum to calculate the corresponding temperature to the measured wavelength. Using Planck's law, the measured temperature is 2.7 K which corresponds to a measured wavelength of 1.06 mm (microwave radiation, as the name Cosmic *Microwave* implies).

In 1991 anisotropies in the CMB were first discovered, by the COBE satellite[3] later earning Smoot and Mather a Nobel prize. As of 2023 the most precise measurements correspond to the Planck experiment in 2018 [1] by the European Space Agency. These anisotropies can be seen in the Fig. 1.1.

---

<sup>3</sup>It will we later discovered that it was not actually uniformly distributed.

Of course, 2.7 K was not the temperature of the plasma at recombination, as it was approximately hotter by a factor  $z = 1090$ , or  $\approx 3000$  K. The reason we measure such smaller temperatures is due to the expansion of the Universe. If today ( $t = t_0$ ) some radiation of wavelength  $\lambda_o$  were observed, that somehow is known to have been traveling for some time  $\Delta t$  will have stretched due to the expansion of the Universe. In other words, the wavelength  $\lambda_e$  of the emitted radiation was smaller by a factor<sup>4</sup>  $a(t')^{-1}$ , with  $t' = t_0 - \Delta t$  being the earlier time at which the radiation was emitted, and defining  $a(t_0) = 1$ . By Wien's displacement law (1.1), this corresponds to a higher temperature by a factor  $a(t')$ . Note this process is normally done backwards: The  $\lambda_e$  is known through spectral lines emission,  $\lambda_o$  is known through measurement and the variable we are interested in is the redshift  $z$ .

Thus, the CMB becomes crucial in explaining the large scale structure of the Universe, since the photons that decoupled from the plasma at recombination wasted more energy leaving denser regions behind losing thermal energy in the process, appearing at a slightly lower temperature (gravitational redshift). On the contrary, those in void regions will appear hotter, being blueshifted. Therefore, temperature fluctuations in the CMB correspond to density fluctuations in the early Universe.

### 1.3. Baryon Acoustic Oscillations

Before recombination, both matter and photons were coupled into the same fluid which we have called the primordial plasma. The particles in the plasma interacted primarily with one another through gravity and the electromagnetic field, depending on the type of matter considered: Ordinary matter known as baryons, and dark matter which will be discussed in Section 1.5.

As already mentioned, matter was not distributed homogeneously. This means that at any point in time before recombination, one could find 'lumps' of dark and baryonic (standard) matter. Combining the restoring force of the gravitational attraction between

---

<sup>4</sup>The factor  $a(t)$  is known as the scale factor of the Universe, and will be explained with further detail later in the work.

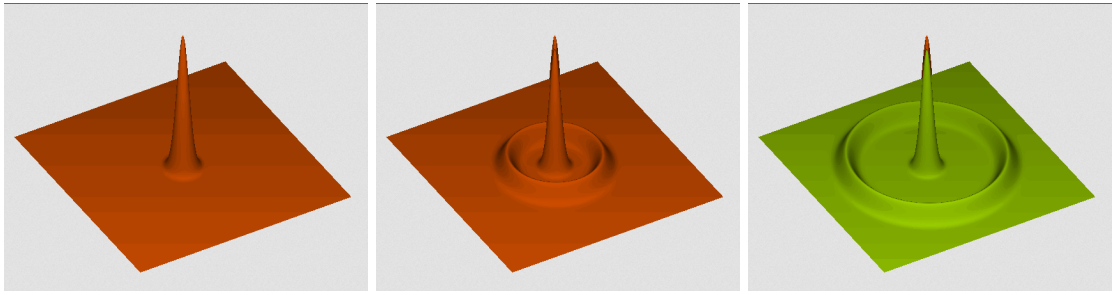


Figure 1.2: Different stages of the Baryon Acoustic Oscillations, as an evolution with time. At first, in the leftmost panel the origin of the oscillations are shown. This is, baryon matter clumped together with dark matter, as a result of the fluctuations of the inflaton field. As the thermal photons from the black body radiation push matter through space, the formed wavefront propagates through space, as seen in the middle panel. After recombination, when the wavelength of the radiation gets sufficiently stretched due to cosmic inflation, the photons do not have enough energy for Thomson Scattering to be effective and thus the oscillations freeze. This stage is shown in the rightmost panel. Courtesy of the diagram: <https://lweb.cfa.harvard.edu/~deisenst/acousticpeak/anim.gif>.

dark and baryonic matter with itself and with one another, and the repulsion caused by the radiation pressure due to the Thomson Effect between baryons and photons, the results are pure acoustic waves propagating through the plasma, with the dark matter lumps being in the center of these waves. Since the baryonic matter is dragged by these sound waves, they are called Baryon Acoustic Oscillations (BAO), and a simplistic explanation of their mechanism is shown in the Fig. 1.2

The waves would propagate throughout the plasma as long as the baryon-photon interaction was strong enough i.e. up to recombination, at which point they froze in time resulting in higher density regions at a fixed distance given by the sound speed of the primordial plasma and the age of the Universe at recombination. Higher density means higher gravitational intensity, which in turn means higher galaxy proliferation in spherical distributions. These spherical distributions (which can be measured in the CMB) are imprinted in the large scale structure of the Universe.

At big enough distances, the radii ( $r_d$ ) of these spheres, also called the sound horizon is used as a standard ‘cosmic ruler’. Cosmological distance measurements are

calculated in terms of  $r_d$ , which is measured from the CMB. This means it needs to be calibrated from external information.  $r_d$  has been measured from the CMB to be around 150 Mpc or 500 million light years. To give an idea of the size of  $r_d$ , the radius of the observable Universe is around 100 times  $r_d$ .

Given the large dimensions of this cosmic ruler and the homogeneity of the Universe on large scales, this ruler is only affected by cosmological expansion rather than late-time gravitational effects. Therefore, it has a constant comoving<sup>5</sup> size throughout the Universe.

These structures were observed for the first time in 2005 simultaneously both by the Sloan Digital Sky Survey[4] and the 2dF Galaxy Redshift Survey[5], the results of which can be seen in the Fig. 1.3. In these pictures one sees the correlation function  $\xi(s)$  and the power spectrum  $P(k)$  (though in the Fig. 1.3 it is called  $W_k$ ). The correlation function  $\xi(r)$ , measures the frequency of the separation distance  $r$  between any two galaxies. If the BAO hypothesis is true, then one would find a local maximum at  $r_d$ , the radius of the frozen spherical waves, which can be seen. These will be the main tools for the study of the BAO, and will be more precisely explained in the chapter 3.

The other tool for studying the BAO is the power spectrum seen in the right panel of the Fig. 1.3. It is, without need of further detail, the Fourier transform of the  $\xi(s)$  function. Indeed, since there is a repeating pattern of wavelength  $r_d$ , one would find local maxima in the spectrum at integer multiples of  $k = 2\pi/r_d$ .

## 1.4. Curvature, dark matter and the expansion of the Universe

After Hubble discovered the expansion of the Universe through Hubble's Law[6]

$$v = H_0 d \quad (1.2)$$

---

<sup>5</sup>'Comoving' meaning the distance one would measure if the expansion of the Universe is factored out.

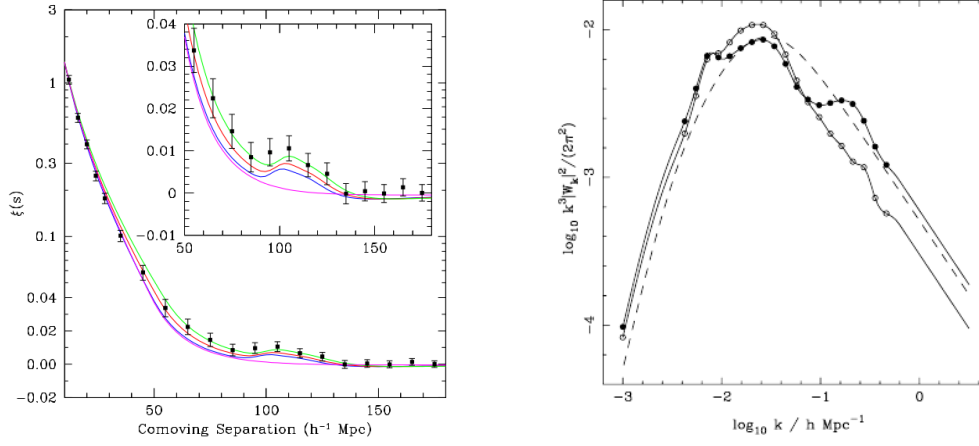


Figure 1.3: The first observations of the Baryon Acoustic Oscillations phenomenon, observed independently by the Sloan Digital Sky Survey (SDSS) [4] as seen in the left panel and the 2dF collaboration [5] in the right panel. These were the main tools that finally determined the existence of the BAO. The SDSS result shows the measured correlation function  $\xi(s)$ . This function represents the distribution of the distance in between any two galaxies. Note the similarity between this graph and the frozen BAO from the Fig. 1.2. The local maximum at  $s \approx 100 \text{ h}^{-1} \text{ Mpc}$  corresponds to the BAO peak. The 2dF result, seen in the rightmost panel is the measured power spectrum  $P(k)$  (here called  $W(k)$ ), which is the Fourier transform of the  $\xi(r)$  function.

with  $v$  the recession speed (the speed at which some point in space is receding only considering the expansion of the Universe),  $H_0 = 100h \text{ km s}^{-1} \text{ Mpc}^{-1}$  Hubble's constant,  $h$  a factor that parametrizes our ignorance on the true value of  $H_0$  (estimated to be around 0.67), and  $d$  the distance of said point, a great deal of studies concerning the expansion of the Universe started. The most relevant result of those for our work are Friedmann's equations

$$H^2(t) := \left(\frac{\dot{a}}{a}\right)^2 = \frac{8\pi G\rho}{3} + \frac{\Lambda c^2}{3} - k\frac{c^2}{a^2} \quad (1.3)$$

$$3\frac{\ddot{a}}{a} = \Lambda c^2 - 4\pi G \left(\rho + \frac{3p}{c^2}\right) \quad (1.4)$$

In these equations we see many new parameters:  $H(t)$  is a generalization of  $H_0$ , where  $H_0$  is the value of  $H(t)$  at the age of the Universe  $t = t_0$ ;  $a(t)$  is already mentioned scale factor of the Universe<sup>6</sup>, meaning that if a certain length measurement  $\Delta x$  was taken at time  $t_1$ , then that same measurement would be  $\frac{a(t_2)}{a(t_1)}\Delta x$  at  $t_2$ ;  $G$  is the Newton's gravita-

<sup>6</sup>More precisely, the Robertson-Walker scale factor [7].



tional constant,  $\rho$  the density of the Universe (including baryonic, dark matter, photons and neutrinos)<sup>7</sup>, and  $\Lambda$  is the cosmological constant which contains information about dark energy, the source of present-time accelerated expansion. Finally we see  $k$ , which is the spatial (Gaussian) curvature of the Universe. This is, asymptotic curvature.

These equations are a consequence of the Friedmann–Lemaître–Robertson–Walker metric [7]

$$ds^2 = -c^2 dt^2 + a^2(t) \left( \frac{dr^2}{1 - kr^2} + r^2 d\theta^2 + r^2 \sin^2 \theta d\phi^2 \right) \quad (1.5)$$

which are a direct result of solutions to Einstein's field equations of General Relativity, which will not be covered in this work. In (1.5) one sees similarities with the usual components in a flat space Minkowskian metric

$$ds^2 = -c^2 dt^2 + dr^2 + r^2 d\theta^2 + r^2 \sin^2 \theta d\phi^2 \quad (1.6)$$

and some new quantities,  $a(t)$  and  $k$ .  $a(t)$  is the aforementioned scale factor, and  $k$  a measure of the curvature of the Universe. It is easier now to see that  $a(t)$  is crucial in the way lengths are measured, being an overall factor in the spatial part that is homogeneous but time-dependent. One can also notice how having different types of Universe affects differently to the metric. For example  $k = 0$  yields (as one would expect from a curvature parameter) a flat Universe.  $k > 0$  corresponds to a Universe with spherical geometry and  $k < 0$  to a Universe of hyperbolic geometry.

If one managed to solve the differential equations in (1.3), the result would be  $a(t)$ , a description of the history of the expansion of the Universe. Moreover, it is also important to notice the relationship between the expansion of the Universe and the distribution of matter in the Universe.

From (1.3) we define the dimensionless density parameter  $\Omega_m$  as  $\frac{\rho}{\rho_c}$ , with the critical density

$$\rho_c = \frac{3H_0^2}{8\pi G} \quad (1.7)$$

which represents the transition point (for a Universe without cosmological constant) between an ever expanding Universe with negative curvature (open Universe) and a

---

<sup>7</sup>In this work, we will only be worried about the coupled baryon-photon fluid around dark matter perturbations.

collapsing Universe with positive curvature (closed Universe). Similarly from the rest of the terms in the equation (1.3) one can define

$$\Omega_\Lambda = \frac{\Lambda c^2}{3H^2}, \Omega_k = -\frac{kc^2}{H^2 a^2} \quad (1.8)$$

$\Omega_\Lambda$  corresponds to the density of dark energy in the Universe, while  $\Omega_k$  is not a density *per se*, but is related to the total energy content of the Universe, determining its curvature. These parameters are what define the certain cosmology we are using, and obey the cosmic sum rule

$$1 = \Omega_m + \Omega_\Lambda + \Omega_k \quad (1.9)$$

Which is just a result of dividing (1.3) evaluated at present time, by  $H_0^2$ .

Historically, the concept of cosmological expansion appeared when Hubble observed that the spectral lines of the nearby galaxies were all shifted towards the red end of the spectrum. Of course, since the Universe is expanding and the distance between two points increases with time, the wavelength of a certain radiation would also be affected by this expansion. This stretching of the wavelength is what is known as *redshift*

$$z = \frac{\lambda_o - \lambda_e}{\lambda_e} = \frac{\lambda_o}{\lambda_e} - 1 \quad (1.10)$$

Being  $\lambda_o$  the observed wavelength and  $\lambda_e$  the emitted wavelength of the considered radiation.  $z$  is a measure of how much the Universe stretched while the radiation traveled, and it can be related to  $a(t)$  through

$$\frac{\lambda_o}{\lambda_e} = 1 + z = \frac{a(t_o)}{a(t_e)} \quad (1.11)$$

Which means that  $z$  is an (dimensionless) variable that admits an interpretation as a time variable, as in an expanding Universe, the scale factor increases with the age of the Universe, therefore the redshift is a decreasing function of the cosmic time.

However, this redshift  $z$  should not be confused with the redshift caused by the Doppler Effect of objects moving away. The processes are different in origin, since cosmological redshift does not need relative movement to shift the radiation towards red wavelengths, it is the expansion of the Universe what stretches the wavelength. On the contrary, the Doppler Effect appears when pulses emitted at regular time are



emitted further away due to the movement of the wave source.

We thus define the comoving distance  $\Delta x'$  of a measurement  $\Delta x$  as

$$\Delta x' = \frac{\Delta x}{a(t)} = (1+z)\Delta x \quad (1.12)$$

i.e. the distance one would have measured had the expansion of the Universe not existed.

With these definitions we can define the observables we are interested in calculating/measuring. Firstly, through (1.3) we calculate  $H(z)$  as

$$H(z) = H_0 \sqrt{\Omega_m(1+z)^3 + \Omega_k(1+z)^2 + \Omega_\Lambda} \quad (1.13)$$

We also define the function of  $z$   $D_H(z)$  known as the Hubble distance

$$D_H(z) = \frac{c}{H(z)} \quad (1.14)$$

Note that  $D_H(z=0) = D_{H,0}$  gives us an idea of the distance at which the recession speed is greater than the speed of light in the vacuum, which is a direct consequence of (1.2).  $D_H$  can also be used to estimate the order of magnitude of the observable Universe.

Through the Hubble distance we define the comoving distance

$$D_C(z) = \int_0^z D_H(z') dz' = \frac{c}{H_0} \int_0^z \frac{dz'}{\sqrt{\Omega_m(1+z')^3 + \Omega_k(1+z')^2 + \Omega_\Lambda}} \quad (1.15)$$

Note  $D_H(z)$  is the derivative of  $D_C(z)$ . From this expression of  $D_C(z)$  one defines the comoving angular diameter distance for some redshift  $z$

$$D_M(z) = \begin{cases} \frac{D_{H,0}}{\sqrt{\Omega_k}} \sinh \left[ \sqrt{\Omega_k} D_C(z) / D_{H,0} \right] & \Omega_k > 0 \\ D_C(z) & \Omega_k = 0 \\ \frac{D_{H,0}}{\sqrt{|\Omega_k|}} \sin \left[ \sqrt{|\Omega_k|} D_C(z) / D_{H,0} \right] & \Omega_k < 0 \end{cases} \quad (1.16)$$

## 1.5. $\Lambda$ Cold Dark Matter model

In the definitions in (1.8) the parameters  $\Omega$  were introduced. This definitions, plus the definition of the density parameter  $\Omega_m$  are part of the set of parameters that form the  $\Lambda$

Cold Dark Matter ( $\Lambda$ CDM) model.

This model is the simplest available way of explaining the current state of the Universe, with six different constants. The name is derived from two of the biggest components of the Universe,  $\Lambda$  (the cosmological constant, related to Dark Energy) and Cold Dark Matter, which is thought to be

- **Cold:** Non relativistic ( $v \ll c$ )
- **Non baryonic:** Made up of non baryonic matter i.e. anything other than protons and neutrons (and by convention, electrons).
- **Disipationless:** Since Dark Matter does not interact with the electromagnetic field, it can not dissipate temperature through photon emission.
- **Collisionless:** Dark matter particles can only interact through gravity and possibly, the weak force and so they do not collide with one another.

The information on this cold dark matter is inside  $\Omega_m$ , since the density  $\rho$  in

$$\Omega_m = \frac{\rho}{\rho_c} = \frac{\rho_b + \rho_{\text{CDM}}}{\rho_c} \quad (1.17)$$

Allowing us to define two new dimensionless density parameters  $\Omega_b = \frac{\rho_b}{\rho_c}$  and  $\Omega_c = \frac{\rho_{\text{CDM}}}{\rho_c}$ , which are part of the six free parameters that define a certain cosmology. These are  $\Omega_b$ ,  $\Omega_c$ ,  $H_0$ , the optical density of reionization  $\tau_{\text{reio}}$ , the amplitude of the primordial power spectrum  $A_s$  and the spectral index of the primordial power spectrum  $n_s$ . Note there is no special choice of parameters, these are just the free parameters chosen for this work. The values for the chosen free parameters are seen in the table 1.1

In this work, an extension of the  $\Lambda$ CDM model is considered. Though the standard cosmological model considers a flat Universe, the curvature parameter will not be fixed to 0 and is therefore allowed to be a free parameter, adding a new degree of freedom to the standard model (not to be confused with the standard model in particle physics). This model could be further extended by considering the mass and number of the neutrinos, generalized models of dark energy, etcetera.

The fiducial (starting) values of these parameters that will be used in this work are the ones seen in table 1.1 From these free parameters, one derives some parameters.

Parameter	Fiducial Value
$\Omega_b$	0.0481
$\Omega_c$	0.2604
$H_0$	67.6 km s <sup>-1</sup> Mpc <sup>-1</sup>
$\tau_{\text{reio}}$	0.09
$A_s$	2.0403·10 <sup>-9</sup>
$n_s$	0.97
$\Omega_k$	[-0.20 , +0.20]
$r_d$	147.784 Mpc
$D_H/r_d$	18.7
$D_M/r_d$	18.3
$\Omega_\Lambda$	[0.49, 0.89]
$\Omega_m$	0.31

Table 1.1: Values of the fiducial cosmological parameters used in the BAO analysis and of the derived values  $r_d$ ,  $D_H/r_d$ ,  $D_M/r_d$ ,  $\Omega_\Lambda$ ,  $\Omega_m$ .

Of those, the main interest is in  $\Omega_\Lambda$ ,  $r_d$ ,  $D_H$ , and  $D_A$ .  $\Omega_\Lambda$  changes with  $\Omega_k$  for a fixed  $\Omega_m$  by the cosmic sum rule (1.9)

$$\Omega_\Lambda = 1 - \Omega_m - \Omega_k \quad (1.18)$$

Thus  $\Omega_\Lambda$  varies between 0.49 and 0.89.

Finally, we define two more parameters  $\alpha_\parallel$  and  $\alpha_\perp$ . These parameters measure the distortion of the measurements in two different directions.  $\alpha_\parallel$  is related to the distortion parallel to the line of sight, and  $\alpha_\perp$ , perpendicular to the line of sight. They are defined by

$$\alpha_\parallel = \frac{[D_H(z)/r_d]}{[D_H(z)/r_d]^{\text{fid}}}, \quad \alpha_\perp = \frac{[D_A(z)/r_d]}{[D_A(z)/r_d]^{\text{fid}}} \quad (1.19)$$

With  $z \simeq 0.698$  being the redshift at which the galaxy measurements were taken.

### Objectives

---

The main objectives of this work are as follows

1. Review the theoretical background of BAO observables, including their physical origin and mathematical formulation, and become familiar with the software tools Rustico, BRASS, and Python for data analysis and visualization.
2. Learn to use these software tools for data preprocessing, analysis, and visualization of BAO-related cosmological data sets, particularly those related to the curvature parameter  $\Omega_k$ .
3. Investigate the impact of different values of  $\Omega_k$  on the behavior of BAO observables.
4. Analyze the most recent observational data on BAO observables, obtained from experiments such as SDSS, BOSS, and eBOSS, and compare the results with theoretical predictions for different values of  $\Omega_k$ .
5. Make use of high performance computing to solve Physics problems.
6. Specific data analysis software development.
7. Learn to control computer clusters via SSH (Secure Shell).

Together, these objectives will provide a comprehensive understanding of the behavior of BAO observables for different values of  $\Omega_k$ , and their role in constraining the curvature parameter and other cosmological parameters.

### Methods and materials.

---

For this work, many different tools were used, which will be categorized in hardware, software and mathematical tools.

In terms of hardware, the author was granted access to the computer facilities of the *FQM-378* research group of the Universidad de Córdoba. Access to these clusters was crucial for the calculations done throughout the work, reducing the time needed for each calculation in several orders of magnitude. Besides the clusters, the author also needed his own personal computer, mainly to remotely access the clusters and also for other types of calculations that could not have been done from the clusters. These calculations include mainly data visualization.

The main mathematical tool for this work was the Fourier Transform [8]. The Fourier Transform is a consequence of Fourier's Theorem. This theorem states that for every 'nice'<sup>8</sup> periodic function  $f(x)$  of period  $L$  one can find a unique linear combination of sine and cosine functions such that

$$f(x) = C + \sum_{n \text{ odd}} a_n \sin\left(\frac{nx}{L}\right) + \sum_{n \text{ even}} b_n \cos\left(\frac{nx}{L}\right) \quad (3.1)$$

---

<sup>8</sup>The conditions for which this theorem does not apply are beyond the scope of this work, and so the 'niceness' of a function need not be defined

With  $C$ ,  $a_n$ ,  $b_n$  given by<sup>9</sup>

$$\begin{cases} C &= \frac{1}{L} \int_L f(x) dx \\ a_n &= \frac{1}{L} \int_L f(x) \sin\left(2\pi \frac{nx}{L}\right) dx, \text{ n odd} \\ b_n &= \frac{1}{L} \int_L f(x) \cos\left(2\pi \frac{nx}{L}\right) dx, \text{ n even} \end{cases} \quad (3.2)$$

This was the original Fourier's result. However this theorem can be expanded to the complex realm as

$$f(x) = \sum_{n=0}^{\infty} c_n e^{i2\pi \frac{nx}{L}}, \text{ with } c_n = \frac{1}{L} \int_L f(x) e^{-i2\pi \frac{nx}{L}} dx \quad (3.3)$$

For each mode  $n$  one can define a new variable  $k = 2\pi n/L$ , leading to the actual definition of the Fourier Transform

$$\tilde{f}(k) = \frac{1}{2\pi} \int_L f(x) e^{-ikx} dx \quad (3.4)$$

In this work, the power spectrum  $P(\mathbf{k})$  is considered, which is the Fourier Transform of the correlation function  $\xi(\mathbf{r})$ . This function, as was already introduced in Section 1.3, is the distribution of the distances at which galaxies are found to be of one another. Since the amount of galaxies present is finite, the data set must then be discrete. This motivates us towards the definition of the Discrete Fourier Transform of a certain data set  $\{(x_i, \xi(x_i))\}_{i=1}^N$

$$P(k_j) = \frac{1}{2\pi} \sum_{i=1}^N e^{-ik_j x_i} \xi(x_i) \quad (3.5)$$

Though one must think that the periodic function hypothesis is being broken, since of course the universe is not made of repeating blocks of the galaxies that surround us. That the universe is infinitely big and repeating is an assumption that needs to be done in order to calculate this Fourier Transform. In other words, these calculations assume periodic boundary conditions.

Another thing to be noted is the fast growing complexity of the algorithm described by (3.5), which grows as  $N^2$ , with  $N$  the number of points used for the calculation. To solve this one would use the Fast Fourier Transform (FFT) [8], instead of the Discrete

---

<sup>9</sup>The subscript in  $\int_L$  only implies the integration over the length  $L$ , since it can be proven that any periodic function  $f(x)$  with period  $L$  verifies  $\int_0^L f(x) dx = \int_a^{L+a} f(x) dx$  for any value of  $a$ . This is, the point at which the integral begins makes no difference, as long as the integration is done over a whole period.

Fourier Transform. This algorithm is based in the decomposition of the space considered with  $N = N_1 N_2$  data points, into two smaller spaces with  $N_1$  and  $N_2$  data points. It then factorizes each problem into smaller problems, and recursively breaks the configuration down into even smaller problems, thus greatly reducing the complexity of the algorithm from  $N^2$  to  $N \log N$ .

The  $P(\mathbf{k})$  has been until now only been vaguely defined. Let  $\rho(\mathbf{x})$  determine the density of galaxies at a given point  $\mathbf{x}$  and  $\bar{\rho}$  the average density throughout the universe. As the interest lays in the fluctuations around the density, it is only natural to be interested in the overdensity  $\delta(\mathbf{x})$  at some position  $\mathbf{x}$

$$\delta(\mathbf{x}) = \frac{\rho(\mathbf{x}) - \bar{\rho}}{\bar{\rho}} \quad (3.6)$$

From this magnitude one calculates the aforementioned correlation function  $\xi(\mathbf{r})$  as<sup>10</sup>

$$\xi(\mathbf{r}) = \langle \delta(\mathbf{x}) \delta(\mathbf{x}') \rangle = \frac{1}{V} \int_V d^3\mathbf{x} \delta(\mathbf{x}) \delta(\mathbf{x} - \mathbf{r}) \quad (3.7)$$

with  $\mathbf{r} = \mathbf{x} - \mathbf{x}'$  And the power spectrum is then defined as its three dimensional Fourier Transform.

To calculate  $P(\mathbf{k})$  one then needs three coordinates for each galaxy (as would be expected from a three dimensional universe). These coordinates will be 2 angular coordinates (the astronomical coordinates declination  $\delta$  and right ascension  $\alpha$ ) and a radial coordinate  $r$  which must be calculated from  $z$ . For this it is necessary to assume a cosmology, since it is what dictates the conversion from redshift to distance through Hubble's law (1.2). For this transformation, the redshift is interpreted as a Doppler shift. At low enough velocities,  $z \approx v/c$  and so (1.2) can be approximated to

$$cz = H_0 r \quad (3.8)$$

The last step to calculate the power spectrum is to interpolate in between each galaxy, similar to how one would build a heat map. This way the catalogue is continuous and no longer discrete. Now, with a continuous density function  $\rho(\mathbf{x})$  all necessities for the power spectrum are met and it can be finally calculated.

---

<sup>10</sup>Note only the dependency on  $r = \|\mathbf{r}\|$  remains, since the universe is (assumed to be) homogeneous and isotropic

All these magnitudes are related to what is called the second moment of the overdensity. In general, the  $n$ th moment  $\mu_n$  of some magnitude  $x$  with a probability distribution  $P(x)$  is defined as

$$\mu_n = \int_{-\infty}^{\infty} x^n P(x) dx \quad (3.9)$$

Though this is done only in one dimension, the definition of the  $n$ th moment of a magnitude  $x$  is easily extended to more dimensions. It should be natural to ask why is only the second moment of the overdensity  $\delta$  considered.<sup>11</sup> It has been measured in the CMB that the universe is a Gaussian field, and these kinds of fields have the property that any moment  $\mu_n$  with  $n \geq 3$  will be 0. These moments (e.g.  $\langle \delta(\mathbf{x})\delta(\mathbf{y})\delta(\mathbf{z}) \rangle$ ) have been shown to all be compatible with 0. This is predicted by the inflation theory, but the strongest reason to believe this is the experimental data.

All these calculations are performed by Rapid foUrier STatistics COde<sup>12</sup> (RUSTICO). This software needs the specific galaxy catalogue to be used, and the statement of the cosmology that is going to be used, in a similar fashion as was done in 1.5. The catalogue to be used in this work is the Luminous Red Galaxy sample from the extended Baryon Oscillation Spectroscopic Survey (LRG eBOSS [9]). With this information it then takes the mentioned steps: Transforms each redshift  $z$  to a radial distance  $r$ , assigns each galaxy to a point  $\mathbf{x}$ , calculates through interpolation the galaxy density at each point  $\rho(\mathbf{x})$ , the overdensity at each point  $\delta(\mathbf{x})$ , the correlation function  $\xi(\mathbf{r})$  and finally its FFT to obtain the power spectrum  $P(\mathbf{k})$ , as seen in the Figure 3.1.

Having the data, it is then necessary to have a model that explains it. The Cosmic Linear Anisotropy Solving System<sup>13</sup>(CLASS) [10] library allows the user to calculate the theoretical curve  $P(k)$  should have for each cosmology. This software takes the corresponding cosmology as an input and returns the power spectrum seen in the leftmost panel of the figure 3.2. Note that this curve looks like a decreasing function which will be named  $P_{\text{smooth}}(k)$ , modulated by an oscillating curve, named  $O_{\text{lin}}(k)$ . These two functions are seen in the middle and rightmost panels respectively, of the figure 3.2,

<sup>11</sup>The dependency on  $\mathbf{x}$  was dropped since  $\delta$  can be both spoken of in configuration space and momentum (Fourier) space. These representations correspond to the  $\xi(\mathbf{r})$  and  $P(\mathbf{k})$  functions, respectively.

<sup>12</sup>Gil-Marín, H. <https://github.com/hectorgil/rustico>

<sup>13</sup>Lesgourgues, J., Tram, T., & Schoenenberg, N. [https://github.com/lesgourg/class\\_public](https://github.com/lesgourg/class_public)



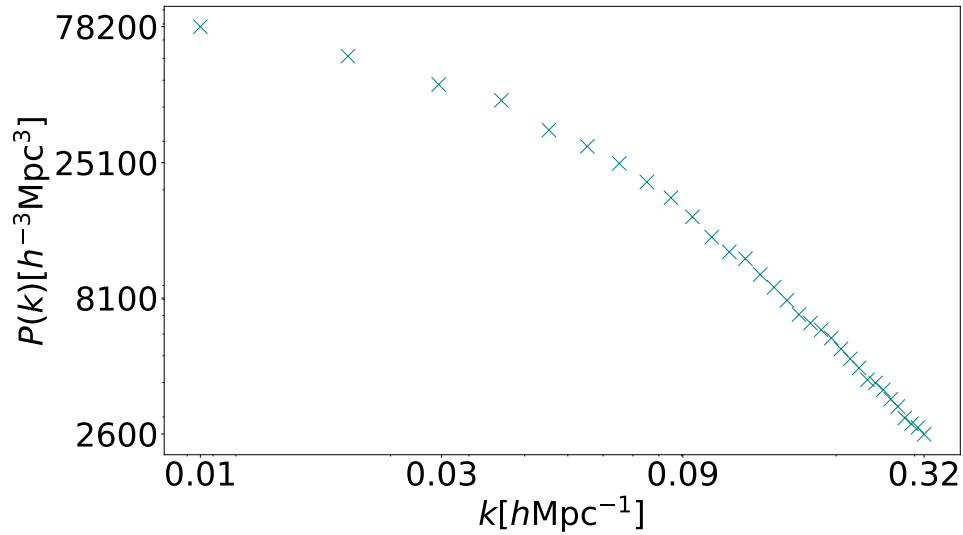


Figure 3.1: The power spectrum  $P(k)$  of the LRG eBOSS [9] catalogue as calculated by RUSTICO assuming a flat universe ( $\Omega_k = 0.00$ )

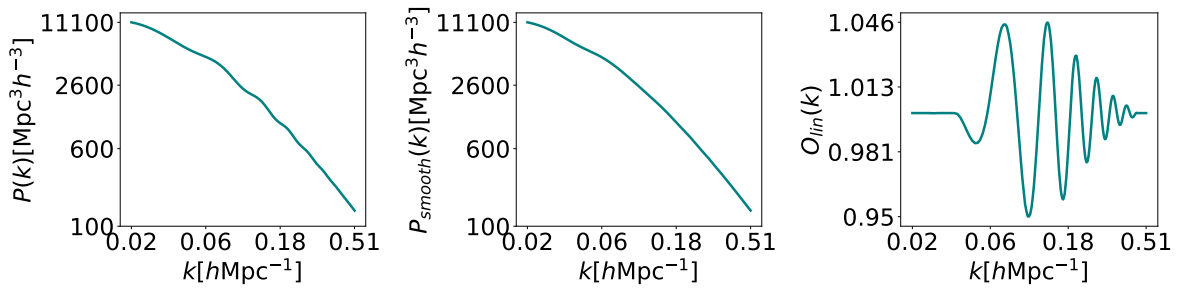


Figure 3.2: Graphic representation of the power spectrum  $P(k)$  as calculated by CLASS (left panel), the smoothed power spectrum  $P_{smooth}(k)$  (middle panel) and the oscillations  $O_{lin}(k)$  (right panel) for a flat universe  $\Omega_k = 0.00$ .

and verify

$$P(k) = P_{smooth}(k)O_{lin}(k) \quad (3.10)$$

To split the power spectrum  $P(k)$  into these two functions, the routine *remove\_bao* from the MontePython project<sup>14</sup> [11] has been used. This routine takes as input the power spectrum  $P(k)$  as an array of points. It then computes the geometrical curvature of the curve and interpolates in between the points at which the calculated curvature results in 0. The output of this function is the smoothed power spectrum  $P_{smooth}(k)$ . By the

<sup>14</sup>Brinckmann T. [https://github.com/brinckmann/montepython\\_public](https://github.com/brinckmann/montepython_public)

definition (3.10), the pure BAO  $O_{\text{lin}}(k)$  are calculated through

$$O_{\text{lin}}(k) = \frac{P(k)}{P_{\text{smooth}}(k)} \quad (3.11)$$

The relationship between the data and the model is analyzed through the Bao and RSD Algorithm for Spectroscopy Surveys<sup>15</sup>(BRASS). This software allows for the calculation of the  $\alpha$  parameters, as defined by (1.19). BRASS takes as input the calculated power spectrum (given by RUSTICO) for some fiducial cosmology, and the theoretical power spectrum for some other fiducial cosmology. It returns, among many other fit parameters, the  $\alpha_{\parallel}$  and  $\alpha_{\perp}$  parameters along with their standard deviations that will allow the calculation of the observables  $D_H/r_s$  and  $D_A/r_s$ . A graphic scheme of the procedure followed throughout this work can be seen in the figure 3.3 and it can be summarized as follows:

1. Starting from a certain galaxy catalogue (in this case, the extended Baryon Oscillation Spectroscopic Survey (eBOSS). This catalogue consists on the astronomical coordinates declination  $\delta$  and right ascension  $\alpha$  of each galaxy and their measured redshift  $z$ .
2. To transform each  $z$  into a radial distance (and therefore its position vector) one needs to assume a fiducial cosmology  $(\Omega_m, \Omega_{\Lambda}, \Omega_k) = (0.31, 0.69 - \Omega_k, \Omega_k)$ . This assumption automatically sets the fiducial values

$$\left[ \frac{D_H}{r_d} \right]^{\text{fid}}, \left[ \frac{D_M}{r_d} \right]^{\text{fid}} \quad (3.12)$$

Through the definitions (1.14) and (1.16).

3. Having the distance from Earth to the galaxies  $r$ , and their angular coordinates  $(\delta, \alpha)$ , their position  $\mathbf{x}$  can be calculated. We now have a discrete distribution  $\rho(\mathbf{x})$  of galaxies. This distribution is then smoothed out, and its overdensity (3.6) calculated.
4. Knowing  $\delta(\mathbf{x})$ , calculate the correlation function  $\xi(\mathbf{r})$  using (3.7).
5. From  $\xi(\mathbf{r})$  calculate the power spectrum  $P(\mathbf{k})$  through its FFT. The steps 3 to 5 are done by RUSTICO.

---

<sup>15</sup>Gil-Marín H. <https://github.com/hectorgil/brass>

6. Generate a fiducial template using CLASS assuming a certain cosmology. In this case, a flat cosmology  $(\Omega_m, \Omega_\Lambda, \Omega_k) = (0.31, 0.69, 0.00)$  that will stay constant for every iteration. Split it into its main components,  $P_{\text{smooth}}(k)$  and  $O_{\text{lin}}(k)$  using the *remove\_bao* routine from MontePython.
7. With the outputs from RUSTICO and CLASS, fit the CLASS template to the RUSTICO data using BRASS, obtaining the best-fit parameters  $\alpha_{\parallel}$  and  $\alpha_{\perp}$  and their corresponding standard deviations.
8. This allows us to obtain the measured observables

$$\frac{D_H}{r_d} = \alpha_{\parallel} \left[ \frac{D_H}{r_d} \right]^{\text{fid}} \quad (3.13)$$

$$\frac{D_M}{r_d} = \alpha_{\perp} \left[ \frac{D_M}{r_d} \right]^{\text{fid}} \quad (3.14)$$

and their corresponding standard deviations.

All of these calculations were done thanks to the clusters to which I was granted access to in the *FQM-378* research group in the Universidad de Córdoba, which had the following specifications:

- 1 node, named Pauli,
- 40 threads for this node, *Intel(R) Xeon(R) Silver 4210R CPU @ 2.40GHz*,
- 64Gb of memory,
- The following Linux version: Ubuntu 22.04.2 LTS, release 22.04 with codename jammy.

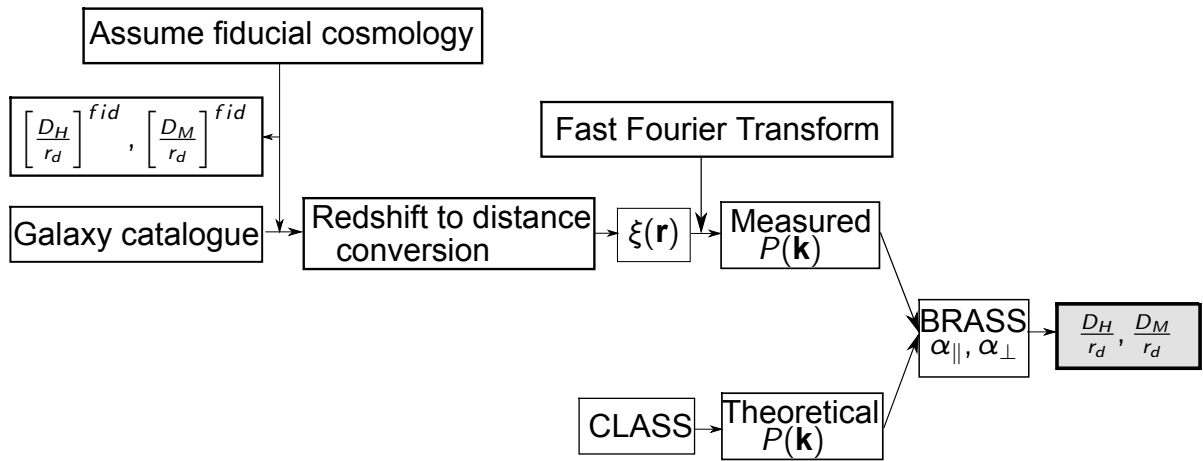


Figure 3.3: The BAO analysis pipeline scheme that was followed throughout this work, that was described along this chapter.

---

## Results

---

Using the tools mentioned in chapter 3, we obtain the data seen in the table 4.1. Firstly, a template power spectrum  $P(k)$  was generated using CLASS. This template stays fixed throughout the calculations, to that of the standard cosmological model. This is, with the six parameters stated in 1.5 and  $\Omega_k = 0.00$ . Having the template, the BAO are removed using the *remove\_bao* routine from Montepython, to obtain exactly the plots seen in 3.2.

For this fixed template, we computed the power spectrum of eBOSS galaxies using the same fiducial cosmology but assuming different values (flat and non-flat) of the curvature parameter  $\Omega_k$  from -0.20 to 0.20, in steps of 0.05. This range covers the curvature values allowed by cosmological observations.

For each one of these  $\Omega_k$ , the software BRASS was used to calculate each corresponding best fitting parameter in the line-of-sight ( $\alpha_{\parallel}$ ) and the transverse ( $\alpha_{\perp}$ ) directions, and its standard deviation. With the  $\alpha$  values calculated, we now know the relation between the fiducial cosmological observables (this is, our initial guess) and the measured value of these observables. In other words,  $\alpha = 1$  would correspond to the case in which the fiducial cosmology corresponded to the cosmology that better fits the data.

These  $\alpha$  values can be seen in the figure 4.1, which presents the  $\alpha_{\parallel}$  and  $\alpha_{\perp}$  on the first row, the fiducial  $D_H/r_d$ ,  $D_M/r_d$  on the second row and the measured  $D_H/r_d$ ,  $D_M/r_d$  for each fiducial cosmology.

$\Omega_k$	$D_H/r_d$	$D_M/r_d$
-0.20	$19.57 \pm 0.85$	$17.85 \pm 0.51$
-0.15	$19.25 \pm 0.84$	$17.85 \pm 0.54$
-0.10	$19.00 \pm 0.80$	$17.96 \pm 0.59$
-0.05	$18.82 \pm 0.77$	$18.13 \pm 0.59$
0.00	$18.66 \pm 0.72$	$18.28 \pm 0.53$
0.05	$18.61 \pm 0.65$	$18.25 \pm 0.47$
0.10	$18.57 \pm 0.61$	$18.24 \pm 0.43$
0.15	$18.50 \pm 0.56$	$18.23 \pm 0.41$
0.20	$18.36 \pm 0.53$	$18.34 \pm 0.39$

Table 4.1: Results of the distance measurements to eBOSS galaxies of the cosmological observables  $D_H/r_d$  and  $D_M/r_d$  assuming different values of the curvature parameter  $\Omega_k$ . Note this table shows the same data as the figure 4.1.

The BRASS calculations were done in an iterative way, which means the output from the software was used as the initial condition for the next iteration. To assure better results three iterations were made for each cosmology. Each iteration for each data point lasted about two hours, which means each data point needed approximately six hours and the whole data set needed a whole forty five hours of computation time.

Both the table 4.1 and the figure 4.1 show the results of the calculation of the different observables for different assumed (fiducial) curvature parameters  $\Omega_k$ . While the table allows us to grasp on the exact values for each measurement, the figure shows the very important tendency of the measurements. Note that the growing tendency of the  $\alpha$  (both parallel and perpendicular) cancels the decreasing tendency of the  $[D/r_d]$  and thus the measured observables stay approximately constant with changes in  $\Omega_k$ . The most important result from these representations is that every measured observable stays within one standard deviation from one another, resulting in compatible results for changes of  $\Omega_k$  in the range  $[-0.20, 0.20]$ .

An example of the data visualization code used in this work is found in the appendix, which shows the code to reproduce the Figure 4.1.

The observable values corresponding to our universe,  $D_H/r_d = 18.66 \pm 0.72$  and  $D_M/r_d = 18.28 \pm 0.53$  must be compared to previous experiments. We see these results are compatible with the bibliography [12]. The measurements ( $D_H/r_d = 19.77 \pm 0.47$  and  $D_M/r_d = 17.65 \pm 0.30$ ) in the mentioned article are done through different methods, and represent the most precise measurements for the redshift range of the SDSS surveys as of 2020.

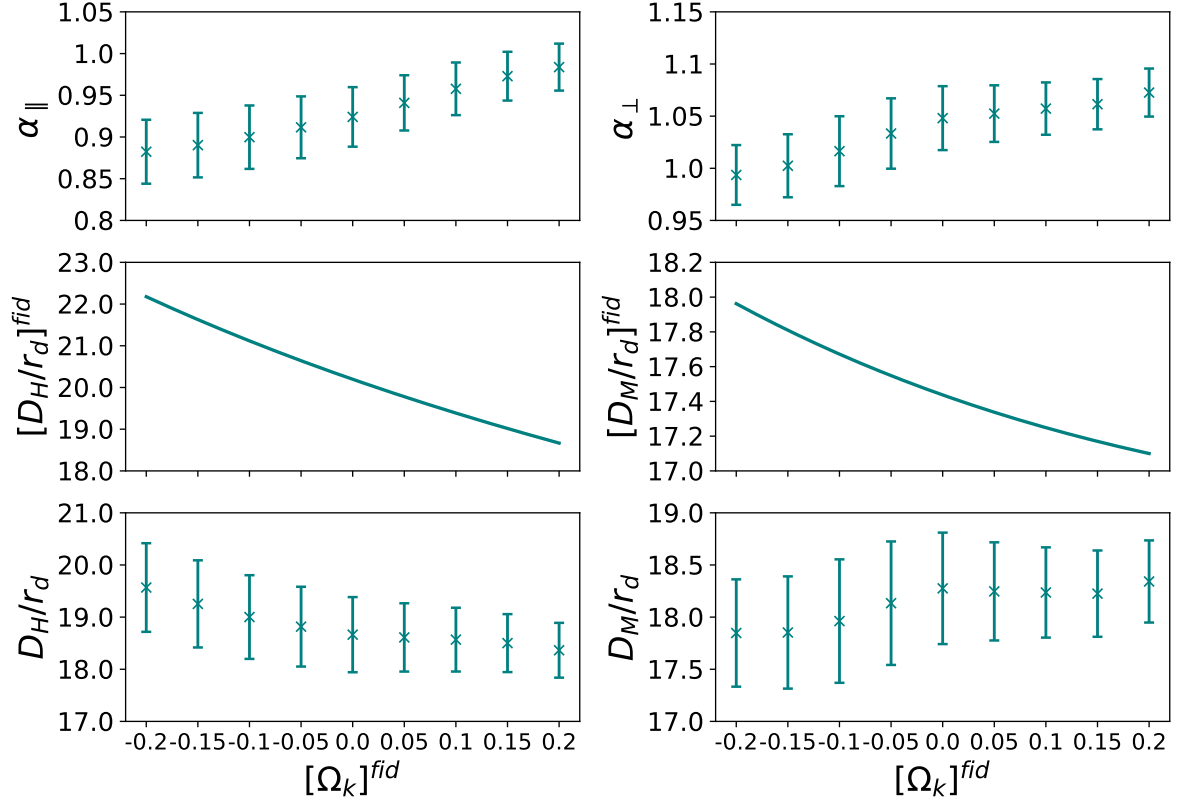


Figure 4.1: Results of the application of the BAO technique to eBOSS galaxies. Top panel: Best fit values and uncertainties on the shifts of the BAO feature in the distribution of galaxies along the line of sight ( $\alpha_{||}$ ) and perpendicular to that direction ( $\alpha_{\perp}$ ) for different values of  $\Omega_k$ . Middle panel: the fiducial distances (Hubble distance and angular diameter distance) as a function of  $\Omega_k$  (with the matter parameter  $\Omega_m = 0.31$ , and the dark energy parameter  $\Omega_{\Lambda} = 1 - \Omega_m - \Omega_k$ , using the equations (1.14) and (1.16)) evaluated at the redshift of eBOSS galaxies. Bottom panel: Best fit values and uncertainties for the Hubble distance and angular diameter distance to eBOSS galaxies for different assumptions on the value of the curvature parameter  $\Omega_k$ , computed as the product of the above two panels. The inferred distances for different values of  $\Omega_k$  are consistent with each other within  $1\text{-}\sigma$ .



### Conclusiones

---

En relación a los objetivos establecidos en el capítulo 2, y considerando los resultados obtenidos en el capítulo 4, se pueden extraer las siguientes conclusiones de este trabajo:

1. Hemos revisado e implementado la metodología de Oscilaciones Acústicas de Bariones (BAO, por sus siglas en inglés) para medir distancias cosmológicas en el Universo, y la hemos aplicado a una muestra de galaxias del Extended Baryon Oscillation Spectroscopic Survey (eBOSS).
2. Hemos utilizado software de cosmología avanzada como CLASS, RUSTICO y BRASS para desarrollar un pipeline que obtiene mediciones de distancia cosmológica de un catálogo de galaxias utilizando la técnica BAO.
3. Además, hemos desarrollado código utilizando la librería Matplotlib escrita en Python para generar visualizaciones de alta calidad de nuestros resultados.
4. Los ordenadores de alto rendimiento del grupo de investigación FQM-378 de la Universidad de Córdoba se han utilizado para calcular la Transformada Rápida de Fourier de la función de correlación de 2 puntos de las galaxias de eBOSS, y para determinar las posiciones de las características de BAO en el espectro de potencia, junto con sus incertidumbres.
5. Suponiendo un modelo cosmológico plano, nuestras mediciones de distancia inferidas a las galaxias de eBOSS (normalizadas a la escala del horizonte de

sonido) son:  $D_H/r_d = 18.66 \pm 0.72$  y  $D_M/r_d = 18.28 \pm 0.53$  para la distancia angular, consistentes con trabajos previos.

6. Nuestro resultado principal es que no hay dependencia significativa de estas observables con respecto a cambios en el valor asumido del parámetro  $\Omega_k$  en el rango de estudio.

Por lo tanto, concluimos que la suposición de un valor particular de  $\Omega_k$  en la conversión de corrimiento al rojo a distancia no tiene ningún efecto significativo (al menos en el rango  $\Omega_k \in [-0.20, +0.20]$ ) en las distancias cosmológicas inferidas a las galaxias de eBOSS utilizando la metodología BAO.

---

### Conclusions

---

Relative to the objectives stated in the chapter 2, and seeing the results obtained in the chapter 4, the following conclusions can be made from this work.

1. We have reviewed and implemented the Baryon Acoustic Oscillation (BAO) methodology to measure cosmological distances in the Universe, and we have applied it to a sample of galaxies from the extended Baryon Oscillation Spectroscopic Survey (eBOSS)
2. We have used advanced cosmology software such as CLASS, RUSTICO and BRASS to develop a pipeline that obtains cosmological distance measurements of a galaxy catalogue using the BAO technique.
3. In addition, we have developed code using the Matplotlib library written in Python to generate quality level visualization of our results.
4. The high performance computers of the University of Cordoba FQM-378 research group have been used to calculate the Fast Fourier Transform of the 2-point correlation function of eBOSS galaxies, and to determine the positions of the BAO features in the power spectrum, together with their uncertainties.
5. Assuming a flat cosmological model, our inferred distance measurements to eBOSS galaxies (normalized to the sound horizon scale) are:  $D_H/r_d = 18.66 \pm 0.72$  and  $D_M/r_d = 18.28 \pm 0.53$  for the angular diameter distance, consistent with previous works.

6. Our main result is that there is no significant dependence of these observables with respect to changes in the assumed value of the  $\Omega_k$  parameter in the range of study.

Therefore, we conclude that the assumption of a particular  $\Omega_k$  value in the redshift-to-distance conversion does not have any significant effect (at least in the range  $\Omega_k \in [-0, 20, +0, 20]$ ) on the inferred cosmological distances to eBOSS galaxies using the BAO methodology.

---

## Bibliography

---

- [1] Planck Collaboration. (2018). Planck 2018 results. VI. Cosmological parameters. *Astronomy & Astrophysics*, 641, A6. <https://doi.org/10.1051/0004-6361/201833910>
- [2] Penzias, A. A., & Wilson, R. W. (1965). A Measurement of Excess Antenna Temperature at 4080 Mc/s. *The Astrophysical Journal*, 142, 419. <https://doi.org/10.1086/148307>
- [3] Smoot, G. F., & Mather, J. C. (1992). Structure in the COBE differential microwave radiometer first-year maps. *The Astrophysical Journal*, 396, L1-L5. <https://doi.org/10.1086/186504>
- [4] Eisenstein, D. J., et al. (The SDSS Collaboration) (2005). Detection of the Baryon Acoustic Peak in the Large-Scale Correlation Function of SDSS Luminous Red Galaxies. *The Astrophysical Journal*, 633, 560-574. <https://doi.org/10.1086/466512>
- [5] Cole, S., et al. (The 2dFGRS Collaboration) (2005). The 2dF Galaxy Redshift Survey: power-spectrum analysis of the final dataset and cosmological implications. *Monthly Notices of the Royal Astronomical Society*, 362, 505-534. <https://doi.org/10.1111/j.1365-2966.2005.09318.x>
- [6] Hubble, E. (1929). A relation between distance and radial velocity among extragalactic nebulae. *Proceedings of the National Academy of Sciences*, 15(3), 168-173. <https://doi.org/10.1073/pnas.15.3.168>
- [7] Weinberg, S. (2008). *Cosmology*, first chapter. OUP Oxford.

- [8] W. H. Press, S. A. Teukolsky, W. T. Vetterling, and B. P. Flannery, “Numerical recipes 3rd edition: The art of scientific computing”, Cambridge University Press, 2007.
- [9] S. Alam *et al.* [eBOSS], Phys. Rev. D **103**, no.8, 083533 (2021) doi:10.1103/PhysRevD.103.083533 [arXiv:2007.08991 [astro-ph.CO]].
- [10] D. Blas, J. Lesgourgues, and T. Tram, “The cosmic linear anisotropy solving system (CLASS). Part II: approximation schemes,” *Journal of Cosmology and Astroparticle Physics*, vol. 2011, no. 07, pp. 034, 2011. <https://doi.org/10.1088/1475-7516/2011/07/034>
- [11] T. Brinckmann and J. Lesgourgues, “MontePython 3: Boosted MCMC sampler and other features,” *Physics of the Dark Universe*, vol. 24, pp. 100260, 2019. <https://doi.org/10.48550/arXiv.1804.07261>
- [12] Héctor Gil-Marín, et al. The Completed SDSS-IV extended Baryon Oscillation Spectroscopic Survey: measurement of the BAO and growth rate of structure of the luminous red galaxy sample from the anisotropic power spectrum between redshifts 0.6 and 1.0. *Monthly Notices of the Royal Astronomical Society*, 498(2):2492–2531, Aug. 2020. URL: <https://arxiv.org/abs/2007.08994>

---

## Appendix: Example of data visualisation code with python & matplotlib

---

```
1 #python 3.9.7
2 #Snippet to plot Fig. 4.1. The other figures were done
3 #in a similar fashion. Firstly, read the alpha values
4 #and their standard deviation (std) from 'logfiles'.
5 #Calculate the fiducial values of the observables through
6 #their definitions in the introduction. Knowing the alpha
7 #values and the fiducial observable, calculate the measured
8 #observables. Each step plots a row in the figure.
9 import numpy as np
10 import matplotlib.pyplot as plt
11 import scipy.constants as ct
12 import util_tools #Library with custom functions
13
14 #Wrapper to make certain function return
15 #an iterable if input was iterable and
16 #return scalar if input was scalar
17 def iterable_output(func):
18     def wrapper(zmax, Ok):
19         try:
20             iter(Ok) #Checks if Ok an array
21             #Calculate by recursion the desired array
22             result = [func(zmax, ok) for ok in Ok]
23             return np.array(result)
24         except TypeError: #input was scalar
25             return func(zmax, Ok)
26     return wrapper
27
28 #Open the desired files
29 files = list(Path('../logfiles_phase2').glob('*3rd*'))
30 #*3rd* as in third iteration, as explained in Chapter 3
31
32 Ok_list = [] #The list of the Omega_k to be used
33 a_para = [] #alpha_parallel list with
34             #each mean and standard deviation
35 a_perp = [] #alpha_perpendicular list with
36             #each mean and standard deviation
37
38 for data in files:
```

```

39     out = util_tools.alpha_from_logfile(data) #Read from Brass output
40     Ok_list.append(out[0])
41     a_para.append(out[1])
42     a_perp.append(out[2])
43
44 n_points = 500
45 Ok_min, Ok_max = min(Ok_list), max(Ok_list)
46 Ok_cont = np.linspace(Ok_min, Ok_max, n_points) #For plotting reasons
47 Ok_rang = Ok_max - Ok_min
48 def H(z, Ok, Om=0.31):
49     return H0*np.sqrt(Om*(1+z)**3 + Ok*(1+z)**2 + 1-Ok-Om)
50
51 #Cosmological observables for a certain cosmology
52 @iterable_output #Wrapper above defined
53 def DH_fid(z, Ok):
54     return ct.c/1000/H(z, Ok) #/1000 factor to match H
55                                #and c units
56 @iterable_output
57 def DC_fid(z, Ok):
58     return sp.integrate.quad(DH_fid, 0, z, args=(Ok,))[0]
59 @iterable_output
60 def DM_fid(z, Ok):
61     DC = DC_fid(z, Ok)
62     DH = DH_fid(z, Ok)
63     if Ok>0:
64         k = DH/np.sqrt(Ok)
65         return k*np.sinh(np.sqrt(Ok)*DC/DH)
66     elif Ok<0:
67         k = DH/np.sqrt(np.abs(Ok))
68         return k*np.sin(np.sqrt(np.abs(Ok))*DC/DH)
69     elif not Ok:
70         return DC
71
72 fig, axes = plt.subplots(3, 2, sharex=True, figsize=(10, 7))
73
74 for Ok, apara, aperp in zip(Ok_list, a_para, a_perp):
75     current_DH = DH_fid(zmax, Ok) * apara[0]/rs
76     current_DH_std = DH_fid(zmax, Ok) * apara[1]/rs
77     current_DM = DM_fid(zmax, Ok) * aperp[0]/rs
78     current_DM_std = DM_fid(zmax, Ok) * aperp[1]/rs
79     axes[0,0].errorbar(Ok, apara[0], yerr=apara[1], fmt='x')
80     axes[0,1].errorbar(Ok, aperp[0], yerr=aperp[1], fmt='x')
81     axes[2,0].errorbar(Ok, current_DH, yerr=current_DH_std, fmt='x')
82     axes[2,1].errorbar(Ok, current_DM, yerr=current_DM_std, fmt='x')
83
84 axes[1,0].plot(Ok_cont, DH_fid(zmax, Ok_cont)/rs)
85 axes[1,1].plot(Ok_cont, DM_fid(zmax, Ok_cont)/rs)
86 axes[0,0].set_ylabel(r'$\alpha_{\parallel}$')
87 axes[0,1].set_ylabel(r'$\alpha_{\perp}$')
88 axes[1,0].set_ylabel(r'$\left[ D_H/r_d \right]^{\{r\}}$')
89 axes[1,1].set_ylabel(r'$\left[ D_M/r_d \right]^{\{r\}}$')
90 axes[2,0].set_ylabel(r'$D_H/r_d$')
91 axes[2,1].set_ylabel(r'$D_M/r_d$')

```



```
92 axes[2,0].set_xlabel(r'$\left[ \Omega_k \right]^{\{r\}}$')
93 axes[2,1].set_xlabel(r'$\left[ \Omega_k \right]^{\{r\}}$')
94 axes[2,0].set_xticks(Ok_list)
95 axes[2,0].set_xticklabels(Ok_list)
96 axes[2,1].set_xticklabels(Ok_list)
97 plt.show()
```